Ronilson Rocha
rocha@em.ufop.br
Federal University of Ouro Preto
EM/DECAT
35400-000 Ouro Preto, MG, Brazil

Gilmar Alves Coutinho
gacoutinho@gmail.com
Federal University of Ouro Preto
EM/DECAT
35400-000 Ouro Preto, MG, Brazil

Alexandre José Ferreira
aleengaut@yahoo.com.br
Federal University of Ouro Preto
EM/DECAT
35400-000 Ouro Preto, MG, Brazil

Flávio Allison Torga
torgautomacao@yahoo.com.br
Federal University of Ouro Preto
EM/DECAT
35400-000 Ouro Preto, MG, Brazil

Multivariable H_2 and H_∞ Control for a Wind Energy Conversion System – A Comparison

The Wind Energy Conversion System (WECS) is a nonlinear system, highly dependent on a stochastic variable characterized by sudden variations, and subjected to cyclical disturbances caused by operational phenomena. Thus, the quality of a WECS controller is measured by its capacity to deal with unmodeled dynamics, stochastic signals, and periodic, as well as non-periodic disturbances. Since the WECS' objectives can be easily specified in terms of maximum allowable gain in the disturbance-to-output transfer functions, H_2 and H_∞ methodologies can be good options for designing a WECS stabilizing controller, combining specifications such as: disturbance attenuation, asymptotic tracking, bandwidth limitation, robust stability, and trade-off between performance and control effort. Designs for WECS multivariable feedback controllers based on H_2 and H_∞ methodologies are presented in this paper. The performances of both controllers are computationally simulated, analyzed and compared in order to identify the advantages and drawbacks of each controller design.

***Keywords**: Wind Energy Conversion System, Control Theory, H_2 and H_∞ control*

Introduction

The reproduction of the current energy scenery is impracticable due to problems to overlap the negative effects associated to progressive use of the conventional resources, such as the inevitable exhaustion of the fossil fuels and the environmental problems. Considering the growing energy demand, the importance of renewable and pollution-free technologies must increase in the future energy strategies. This fact has attracted great interest in the development of Wind Energy Conversion Systems (WECS).

The basic configuration of a WECS is a wind turbine (WT) coupled to an electric generator, either directly or by a gear-box. In spite of its simplicity, WECS represents an interesting control problem. Due to difficulty in physical phenomena characterizing by means of experimental investigation, WECS modeling becomes a complex problem. The aerodynamic characteristics of a WT are nonlinear and highly dependent on wind speed, which is characterized by sudden variations and behaves simultaneously as energy supply and disturbance signal. A ripple torque is introduced into WECS by operational phenomena such as tower shadow, wind shear, yaw misalignment and shaft tilt (Freris, 1990). The speed and/or power control of a WECS can be achieve by adjusting the generator torque (Novak et al., 1995) or varying the pitch angle of the blades in some WT configurations (Wasynczuk et al., 1981). Thus, a WECS is a nonlinear multivariable system, in which the control system has to deal with several uncertainties, parameter variations, nonlinearities, noise, unmodeled dynamics, periodic and non-periodic disturbances.

In this context, the quality of a WECS control system is measured by its stochastic properties and its capacity to establish a trade-off between detrimental dynamic load reduction and energy conversion maximization, shaping the system dynamics in order to satisfy performance and stability specifications (Leithead et al., 1991). Another important control objective is to reduce the influence of wind fluctuation and ripple torque at any rotation speed, because these cause large power fluctuations and unavoidable vibrations with detrimental effects to WECS (Dessaint et al., 1986). The classic methods do not offer a completely satisfactory solution to WECS control design, resulting in controllers that do not offer the necessary robustness for both stability and performance (Dessaint et al., 1986; Lefebvre and Dubé, 1988; Leithead et al., 1991). Considering that the WECS control objectives can be easily specified in terms of maximum allowable gain in the disturbance-to-output transfer functions, H_2 and H_∞ methodologies can be good options for designing a WECS stabilizing controller, since both approaches combine specifications, such as: disturbance attenuation, asymptotic tracking, bandwidth limitation, robust stability and trade-off between performance and control effort. The H_2 methodology is particularly appropriate in situations where disturbance rejection and noise suppression are important, while H_∞ is usually preferred when the robustness to plant uncertainties is the dominant issue (Maciejowski, 1989; Skogestad and Postlethwaite, 2001).

The designs of multivariable feedback controllers based on H_2 and H_∞ methodologies are presented in this paper. The structure shown in Fig. 1 was used for the rotation control for an upwind variable-pitch horizontal axis WT (HAWT) coupled to an induction generator, which is connected to the electric network via power electronic converters. The performances of both controllers are computationally simulated, analyzed and compared so as to identify advantages and drawbacks of each design.

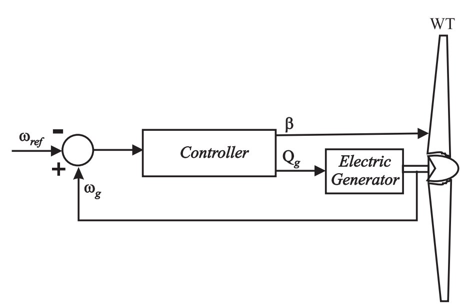

Figure 1. Multivariable structure for a WECS rotation feedback control system.

Paper accepted October, 2010. Technical Editor: Glauco Caurin.

WECS Model

A nonlinear model of a WECS with suitable complexity was developed for computational simulations. Five distinct WECS subsystems are considered in this modeling: wind, aerodynamics, drive train, pitch actuator and generator.

Wind

The WECS operation is highly dependent on wind speed, a stochastic variable characterized by sudden variations which simultaneously behaves as the energy supply and disturbance signal. Although the wind is a multidimensional stochastic process that depends on time and spatial coordinates, a two-dimensional model is generally enough to evaluate the dynamics of WECS (Wasynczuk et al., 1981). Due to a phenomenon known as "wind shear"', wind speed depends on height. Its value V_i at the representative point 3/4 of the cord of i-th blade at instant t is given by (Golding, 1977; Wasynczuk et al., 1981; Freris, 1990):

$$V_i = V_H\left[1+\frac{3}{4}\frac{R}{H}\sin(\theta)\right]^a \tag{1}$$

where a is a coefficient that depends on local topography, θ_i is the spatial angle of the i-th blade, R is the WT radius, and H is the height of the tower that supports the WT. The wind speed V_H at height H can be described by four components (Rohatgi and Pereira, 1996; Leith and Leithead, 1997):

$$V_H = \overline{V} + V_G + V_R + \Delta V \tag{2}$$

where $\overline{V}$ is the effective average wind speed at height H. The discrete longitudinal wind gust V_G at instant t can be described as (Hwang and Gilbert, 1978; Anderson and Bose, 1983; Raina and Malik, 1985):

$$V_G = \frac{3\overline{V}}{2\ln\left(\frac{H}{h_o}\right)}\left[1-\exp\left(-\frac{\overline{V}\Delta T_G}{1.48H}\right)\right]^{\frac{1}{2}}\left[1-\cos\left(2\pi\frac{t-T_G}{\Delta T_G}\right)\right] \tag{3}$$

where T_G is the instant when the gust begins, ΔT_G is the gust duration, and h_o is a parameter known as roughness height. Another kind of sudden wind speed variation considered in this modeling is the ramp component V_R, which is given by (Anderson and Bose, 1983):

$$V_R = V_{RMAX}\left(\frac{t-T_R}{\Delta T_R}\right) \tag{4}$$

where V_{RMAX} is the peak of the ramp, T_R is the instant when the ramp begins and ΔT_R is the ramp duration. For small ΔT_R, the ramp component can be used as an approach to the wind step. The wind speed stochastic component is the wind fluctuation ΔV, which can be estimated as (Wasynczuk et al., 1981):

$$\Delta V = 2\sum_{i=1}^{N}\left[S_v(\psi_i)\Delta\omega\right]^{\frac{1}{2}}\cos(\psi_i t+\phi_i) \tag{5}$$

where $\psi_i = (i\text{-}1/2)\Delta\psi$, ϕ_i is an independent random variable with uniform density in the interval of 0 to 2π, and $S_v(\psi_i)$ is a power spectral density given by:

$$S_v(\psi_i) = \frac{2K_N F^2|\psi_i|}{\pi^2\left[1+\left(\frac{F\psi_i}{\mu\pi}\right)^2\right]^{\frac{4}{3}}} \tag{6}$$

where K_N is the superficial drag coefficient, F is the turbulence scale, and μ is the mean wind speed at the reference height. For good results, it is suggested that $N = 50$ and $\Delta\psi$ be between 0.5 and 2.0 rad/s (Anderson and Bose, 1983).

WT Aerodynamics

The aerodynamics of a WT is normally described by dimensionless coefficients, which define the WT ability to convert kinetic energy of moving air into mechanical power C_p or torque C_q (Novak et al., 1995; Medeiros et al., 1996). Both coefficients C_p and C_q depend on the constructive aspects of the WT blades and they are nonlinear functions of pitch angle β, yaw angle θ and a parameter known as tip-speed ratio λ, which is defined for the i-th blade of WT as:

$$\lambda_i = \frac{R\omega_i}{V_i} \tag{7}$$

where ω_i is the rotation of the WT i-th blade. Admitting that the WT is always aligned with the wind direction (θ=0^o), the aerodynamic torque Q_{ai} of the WT's i-th blade is given by (Wasynczuk et al., 1981; Freris, 1990; Novak et al., 1995):

$$Q_{ai} = \frac{1}{2}\rho\pi R^3\frac{C_p(\lambda_i,\beta)}{\lambda_i}V_i^2 = \frac{1}{2}\rho\pi R^3 C_q(\lambda_i,\beta)V_i^2 \tag{8}$$

where ρ = air density.

Pitch Actuator

Some WTs have an electro-hydraulic device to adjust the pitch angle β of its blades, which can be modeled as (Johnson and Smith, 1976):

$$\tau^2\frac{d^2\beta}{dt^2} + 2\xi\tau\frac{d\beta}{dt} + \beta = \beta_c \tag{9}$$

where β_c is the command signal, τ is the time constant of the pitch actuator and ξ is the damping factor.

Drive Train

The drive train of a WECS can be modeled as a set of masses connected by flexible shafts according to the block diagram shown in Fig. 2 (Novak et al., 1995; Hori et al., 1999). Admitting an ideal gear-box, the mechanical coupling system of a WT with n blades can be described by the classical rotational dynamics:

- i-th blade:

$$J_i\dot{\omega}_i + D_i\omega_i = Q_{ai} - D_{ih}(\omega_i-\omega_t) - Q_{mih} \tag{10}$$

- hub:

$$J_h\dot{\omega}_h + D_h\omega_h = \sum_{i=1}^{n}\left[D_{ih}(\omega_i-\omega_t)-Q_{mih}\right] - D_{hg}(\omega_t-\omega_g) - Q_{mhg} \tag{11}$$

- generator:

$$J_g \dot{\omega}_g + D_g \omega_g = D_{hg}\left(\omega_t - \omega_g\right) + Q_{mhg} - Q_g \tag{12}$$

- shaft torques:

$$\dot{Q}_{mih} = K_{ih}\left(\omega_i - \omega_t\right) \tag{13}$$

$$\dot{Q}_{mhg} = K_{hg}\left(\omega_t - \omega_g\right) \tag{14}$$

where ω_t = hub rotation, ω_g = generator rotation, J_i = i-th blade inertia, J_h = hub inertia, J_g = generator inertia (including gear-box inertia), D_i = i-th blade damping, D_h = hub damping, D_g = generator damping, D_{ih} = i-th blade-hub connection damping, D_{hg} = shaft damping, K_{ih} = i-th blade-hub connection stiffness, K_{hg} = shaft stiffness, Q_{mih} = i-th blade torque, Q_{mhg} = shaft torque and Q_g = generator torque.

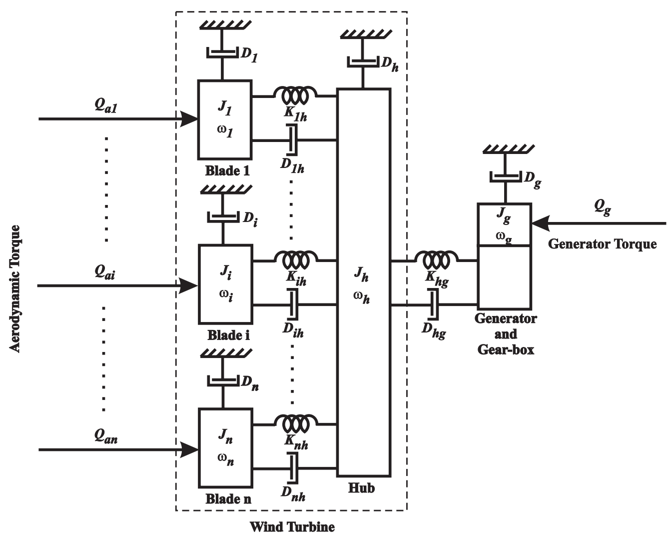

Figure 2. WECS model for simulation.

Generator Torque

The electric generator converts the rotational mechanical energy of the WT into electric energy for costumers. For variable speed WECSs, the electric generator must be connected to the grid using power electronic converters. In this case, the generator torque is independent of the WECS dynamics (Novak et al., 1995) and can be considered as a system input in the WECS model. Since the dynamics of electric systems are extremely fast if compared to drive train dynamics, a quasi-static model is assumed for the electric generator.

Controller Design for WECS

Nominal Linear Model

In order to design H_2 or H_∞ controllers, it is necessary to obtain a nominal linear model for the WECS. In the nonlinear C_pxλ and C_qxλ characteristics of a WT for $\beta = 0^o$, which is shown in Fig. 3, it is possible to identify two distinct regions in the WT operation. The stall region (A) is characterized by a positive slope, resulting in an unstable operation with sudden and significant drops in the aerodynamic torque. The stable operational region (B) is characterized by a negative slope, corresponding to normal WT operation, where the aerodynamic torque Q_a can be linearized as (Novak et al., 1995; Rocha et al., 2001; Rocha and Martins Filho, 2003):

$$\dot{Q}_a = \alpha \dot{V} + \gamma \dot{\omega}_t + \kappa \dot{\beta} \tag{15}$$

where α is a scaling factor for torque disturbance due to wind variations $\dot{V}$, γ denotes feedback speed coefficient from the drive train, and κ represents the pitch control gain. In steady state, $\dot{V}$ is the wind fluctuation ΔV, which can be assumed for design purposes as a white noise with zero mean (Wasynczuk et al., 1981). Since it is desirable to operate at maximum C_p, the aerodynamic torque linearization can be performed in the corresponding λ_{opt}, which is always situated in the normal operation region. Considering $\overline{V}_{nom}$ as the nominal wind speed on the WECS location, the coefficients α, γ, and κ can be easily computed from WT data as:

$$\alpha = \left.\frac{\partial Q_a}{\partial V}\right|_{\lambda_{opt},\beta=0^o} = \frac{3}{2}\rho A R \frac{C_{p_{opt}}}{\lambda_{opt}} \overline{V}_{nom} \tag{16}$$

$$\gamma = \left.\frac{\partial Q_a}{\partial \omega_t}\right|_{\lambda_{opt},\beta=0^o} = -\frac{1}{2}\rho A R^2 \frac{C_{p_{opt}}}{\lambda_{opt}^2} \overline{V}_{nom} \tag{17}$$

$$\kappa = \left.\frac{\partial Q_a}{\partial \beta}\right|_{\lambda_{opt},\beta=0^o} = \frac{1}{2}\rho A R \overline{V}_{nom}^2 \left.\frac{\partial C_q}{\partial \beta}\right|_{\lambda_{opt},\beta=0^o} \tag{18}$$

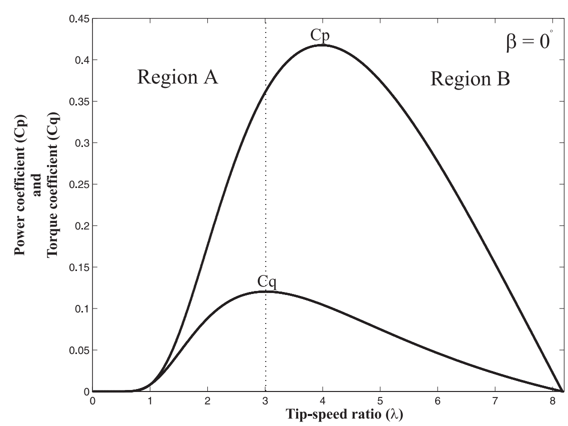

Figure 3. Aerodynamic characteristics of a WT.

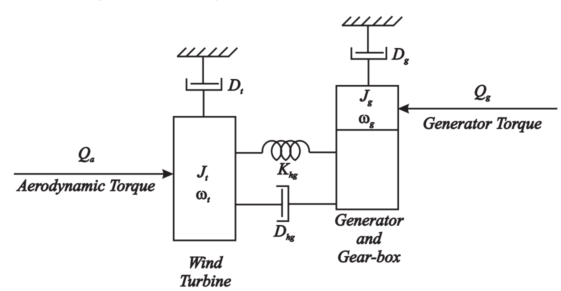

Figure 4. WECS model for control design.

Although a real mechanical drive train has rigid disks, flexible shaft elements with distributed mass and stiffness, an approximated two-mass model shown in Fig. 4 is enough to design a controller for WECS (Freris, 1990; Novak et al., 1995). Admitting an ideal gear-box and reducing all quantities to the primary side, the mechanical coupling can be described as (Leith and Leithead, 1997):

$$J_t\dot{\omega}_t + D_t\omega_t = Q_a - Q_{mhg} - D_{hg}\left(\omega_t - \omega_g\right) \tag{19}$$

$$J_g\dot{\omega}_g + D_g\omega_g = D_{hg}\left(\omega_t - \omega_g\right) + Q_{mhg} - Q_g \tag{20}$$

$$\dot{Q}_{mhg} = K_{hg}\left(\omega_t - \omega_g\right) \tag{21}$$

where J_t is the total WT inertia, and D_t = total WT damping.

The linearized equations 15, 19, 20 and 21 constitute the nominal linear state model of a pitch regulated WT. One of the control inputs is the generator torque Q_g, which represents the electric load mechanically connected to generator. It is adjustable and virtually independent from WECS dynamics (Novak et al., 1995). The second control input is the pitch angle β, which greatly impacts the control system due to its active influence on the WT's aerodynamic efficiency. In this context, WECS configures a multivariable system.

Since the dynamics of the pitch actuator is very fast if compared to WT dynamics, it can be considered as an unmodeled uncertainty to avoid an unnecessary increase in the state variables of the nominal model, resulting in a simplest controller with the smallest order. The structural dynamics of the blades and tower are also considered as unmodeled uncertainties in this approach.

Control Objectives

Aiming to explicit the trade-off between the control requirements, the nominal model has to be manipulated using weighting functions to obtain a generalized system $\mathbf{G}(s)$ shown in Fig. 5, given by:

$$\mathbf{G}(s) = \begin{cases} \dot{\mathbf{x}} = \mathbf{A}\mathbf{x} + \mathbf{B_1}\mathbf{w} + \mathbf{B_2}\mathbf{u} \\ \mathbf{z} = \mathbf{C_1}\mathbf{x} + \mathbf{D_{11}}\mathbf{w} + \mathbf{D_{12}}\mathbf{u} \\ \mathbf{y} = \mathbf{C_2}\mathbf{x} + \mathbf{D_{21}}\mathbf{w} + \mathbf{D_{22}}\mathbf{u} \end{cases} \tag{22}$$

where $\mathbf{x}$ = state vector, $\mathbf{u}$ = control signals, $\mathbf{w}$ = exogenous inputs, $\mathbf{z}$ = control objectives outputs and $\mathbf{y}$ = measured outputs. The exogenous inputs $\mathbf{w}$ are signals determined by external processes or environments that influence the dynamics of the system, such as reference signals, commands, disturbances and noises.

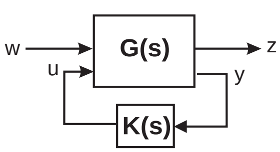

Figure 5. Generalized system.

The main control requirement of WECS is to reduce detrimental dynamic loads on the shaft, which is obtained by minimization of the shaft torque variations over all bandwidth. In this context, the first control objective output z_1 is obtained by weighting the difference $\Delta\omega = \omega_t - \omega_g$ with a fixed gain K_δ. Another important control requirement for fixed and variable speed WECS is the WT rotation control, which can be defined as the reduction of the rotation error $e_t = \omega_{sp} - \omega_t$. Thus, the second control objective output z_2 is generated by weighting e_t with a PI function:

$$K_e(s) = \frac{z_2(s)}{e_t(s)} = K_p + \frac{K_i}{s} \tag{23}$$

which implies in the augmentation of the original nominal model with an integrator. The control design has to minimize the effects of wind fluctuation and ripple torque over the energy delivered to electric load, generating the third control objective output z_3, which is obtained by weighting the generator torque Q_g with a fixed gain K_q. Finally, it is necessary to limit the bandwidth of pitch control input β by weighting it with a fixed gain K_β. The exogenous inputs $\mathbf{w}$ on WECS are the rotation reference ω_{sp} and wind fluctuation $\dot{V}$. Due to practical constraints relative to the assembly, cost and maintenance of the sensors, the generator rotation ω_g is considered the only measured output y. Considering $\mathbf{u} = [Q_g\ \beta]'$, $\mathbf{w} = [\omega_{sp}\ \dot{V}]'$ and $\mathbf{x} = [Q_a\ \omega_t\ \omega_g\ Q_{mhg}\ \int e_t dt]'$, the nominal WECS model augmented with weighting functions is given by:

$$\dot{\mathbf{x}} = \begin{bmatrix} \frac{\gamma}{J_t} & -\frac{\gamma(D_t + D_{hg})}{J_t} & \frac{\gamma D_{hg}}{J_t} & -\frac{\gamma}{J_t} & 0 \\ \frac{1}{J_t} & -\frac{D_t + D_{hg}}{J_t} & \frac{D_{hg}}{J_t} & -\frac{1}{J_t} & 0 \\ 0 & \frac{D_{hg}}{J_g} & -\frac{D_{hg} + D_g}{J_g} & \frac{1}{J_g} & 0 \\ 0 & K_{hg} & -K_{hg} & 0 & 0 \\ 0 & -1 & 0 & 0 & 0 \end{bmatrix}\mathbf{x} + \begin{bmatrix} 0 & \alpha \\ 0 & 0 \\ 0 & 0 \\ 0 & 0 \\ 1 & 0 \end{bmatrix}\mathbf{w} + \begin{bmatrix} 0 & \kappa \\ 0 & 0 \\ -\frac{1}{J_g} & 0 \\ 0 & 0 \\ 0 & 0 \end{bmatrix}\mathbf{u} \tag{24}$$

$$\mathbf{z} = \begin{bmatrix} 0 & K_\delta & -K_\delta & 0 & 0 \\ 0 & -K_p & 0 & 0 & K_i \\ 0 & 0 & 0 & 0 & 0 \\ 0 & 0 & 0 & 0 & 0 \end{bmatrix}\mathbf{x} + \begin{bmatrix} 0 & 0 \\ K_p & 0 \\ 0 & 0 \\ 0 & 0 \end{bmatrix}\mathbf{w} + \begin{bmatrix} 0 & 0 \\ 0 & 0 \\ K_q & 0 \\ 0 & K_\beta \end{bmatrix}\mathbf{u} \tag{25}$$

$$y = \begin{bmatrix} 0 & 0 & -1 & 0 & 0 \end{bmatrix}\mathbf{x} + \begin{bmatrix} 1 & 0 \end{bmatrix}\mathbf{w} + \begin{bmatrix} 0 & 0 \end{bmatrix}\mathbf{u} \tag{26}$$

H$_2$ Methodology

The H$_2$ controller design can be formalized as an optimization problem, where the goal is to find a controller $\mathbf{K}_2$ that internally stabilizes the system $\mathbf{G}(s)$, so that H$_2$ norm:

$$\left\|\mathbf{H}_{zw}\right\|_2 = \sqrt{\frac{1}{2}\int_{-\infty}^{+\infty}\left[\mathbf{H}_{zw}(j\omega)\mathbf{H}_{zw}^H(-j\omega)\right]d\omega} \tag{27}$$

is minimized, where $\mathbf{H}_{zw}$ denotes the transfer function matrix from exogenous inputs $\mathbf{w}$ to objective outputs $\mathbf{z}$. This H$_2$ optimization problem is equivalent to the conventional LQG problem (Skogestad and Postlethwaite, 2001) involving a cost function:

$$J = \int_0^\infty \begin{bmatrix} \mathbf{x}' & \mathbf{u}' \end{bmatrix} \begin{bmatrix} \mathbf{C}_1'\mathbf{C}_1 & \mathbf{C}_1'\mathbf{D}_{12} \\ \mathbf{D}_{12}'\mathbf{C}_1 & \mathbf{D}_{12}'\mathbf{D}_{12} \end{bmatrix} \begin{bmatrix} \mathbf{x} \\ \mathbf{u} \end{bmatrix} dt \tag{28}$$

with correlated white noises ξ (states) and η (measurements) entering in the system via $\mathbf{w}$ channel associated with the correlation function:

$$E\left\{\begin{bmatrix} \xi(\tau)\xi'(\tau) & \xi(\tau)\eta'(\tau) \\ \eta(\tau)\xi'(\tau) & \eta(\tau)\eta'(\tau) \end{bmatrix}\right\} = \begin{bmatrix} \mathbf{B}_1\mathbf{B}_1' & \mathbf{B}_1\mathbf{D}_{12}' \\ \mathbf{D}_{12}\mathbf{B}_1' & \mathbf{D}_{12}\mathbf{D}_{12}' \end{bmatrix}'\delta(t-\tau) \tag{29}$$

This problem can be solved by the resolution of the following two Riccati equations

$$\mathbf{Y}_2\mathbf{A}' + \mathbf{A}\mathbf{Y}_2 - \mathbf{Y}_2\mathbf{C}_2'\mathbf{C}_2\mathbf{Y}_2 + \mathbf{B}_1\mathbf{B}_1' = 0 \tag{30}$$

$$\mathbf{A}'\mathbf{X}_2 + \mathbf{X}_2\mathbf{A} - \mathbf{X}_2\mathbf{B}_2\mathbf{B}_2'\mathbf{X}_2 + \mathbf{C}_1\mathbf{C}_1' = 0 \tag{31}$$

resulting in an H$_2$ optimal controller $\mathbf{K}_2(s)$ given by:

$$\mathbf{K}_2(s) = \begin{cases} \dot{\hat{\mathbf{x}}} = \left(\mathbf{A} - \mathbf{B}_2\mathbf{B}_2'\mathbf{X}_2 - \mathbf{Y}_2\mathbf{C}_2'\mathbf{C}_2\right)\hat{\mathbf{x}} + \mathbf{Y}_2\mathbf{C}_2'y \\ \mathbf{u} = -\mathbf{B}_2'\mathbf{X}_2\hat{\mathbf{x}} \end{cases} \tag{32}$$

H_∞ Methodology

Feedback control design can be also formalized in terms of H_∞ norm optimization. The sub-optimal H_∞ control problem is to find all admissible compensators $\mathbf{K}_\infty(s)$ which internally stabilize the generalized system $\mathbf{G}(s)$ and minimize the norm (Doyle et al., 1989):

$$\|\mathbf{H}_{zw}\|_\infty = \sup_\omega \bar{\sigma}[\mathbf{H}_{zw}] \tag{33}$$

such that $\|\mathbf{H}_{zw}\|_\infty < \varepsilon$. Considering $\mathbf{D}_{11} = 0$ and $\mathbf{D}_{22} = 0$, the solution of this problem can be given by:

$$\mathbf{K}_\infty(s) = \begin{cases} \dot{\hat{\mathbf{x}}} = (\mathbf{A}_\infty - \mathbf{B}_2\mathbf{B}_2'\mathbf{X}_\infty - \mathbf{L}_\infty\mathbf{C}_2)\hat{\mathbf{x}} + \mathbf{L}_\infty y \\ \mathbf{u} = -\mathbf{B}_2'\mathbf{X}_\infty\hat{\mathbf{x}} \end{cases} \tag{34}$$

where

$$\mathbf{A}_\infty = \mathbf{A} + \varepsilon^{-2}\mathbf{B}_1\mathbf{B}_1'\mathbf{X}_\infty \tag{35}$$

$$\mathbf{L}_\infty = (\mathbf{I} - \varepsilon^{-2}\mathbf{Y}_\infty\mathbf{X}_\infty)^{-1}\mathbf{Y}_\infty\mathbf{C}_2' \tag{36}$$

and $\mathbf{X}_\infty$ and $\mathbf{Y}_\infty$ are the solutions for two Riccatti equations:

$$\mathbf{A}'\mathbf{X}_\infty + \mathbf{X}_\infty\mathbf{A} - \mathbf{X}_\infty\mathbf{B}_\infty\mathbf{B}_\infty'\mathbf{X}_\infty + \mathbf{C}_1'\mathbf{C}_1 = 0 \tag{37}$$

$$\mathbf{Y}_\infty\mathbf{A} + \mathbf{A}'\mathbf{Y}_\infty - \mathbf{Y}_\infty\mathbf{C}_\infty'\mathbf{C}_\infty\mathbf{Y}_\infty + \mathbf{B}_1\mathbf{B}_1' = 0 \tag{38}$$

where

$$\mathbf{B}_\infty\mathbf{B}_\infty' = \varepsilon^{-2}\mathbf{B}_1\mathbf{B}_1' - \mathbf{B}_2\mathbf{B}_2' \tag{39}$$

$$\mathbf{C}_\infty\mathbf{C}_\infty' = \varepsilon^{-2}\mathbf{C}_1\mathbf{B}_1' - \mathbf{C}_2\mathbf{C}_2' \tag{40}$$

The existence of a solution for H_∞ control problem is assured by the following conditions: $\mathbf{X}_\infty \geq 0$, $\mathbf{Y}_\infty \geq 0$ and the eigenvalues $\rho(\mathbf{X}_\infty\mathbf{Y}_\infty) \leq \varepsilon^2$. The best solution for sub-optimal/optimal H_∞ controller can be computed using the loop-shifting two-Riccatti formulae (Chang and Safonov, 1996).

Simulation Results

Plant Description

The WECS considered in this paper consists of an upwind Horizontal Axis WT coupled to a 2.5MW four-pole electric generator by a gear-box (ratio 1:102.5) as shown in Fig. 6 (Wasynczuk et al., 1981). This WT has two blades (NACA230XX series airfoil), each one with a length of 45.72 m, where the outer 30% corresponds to the variable-pitch section controlled by a servo-hydraulic actuator. The generator and other support equipment are enclosed in a nacelle, which is mounted atop a tower with 60.96 m where wind measurements are performed. A yaw control allows the correct alignment of the WT rotor with the wind direction. The complex nonlinear and stochastic mathematical model presented in the section "WECS Model" is used to simulate this WECS, while the nominal model described in the subsection "Nominal Linear Model" is used to design the controllers. The scheme for dynamic simulation for this closed-loop WECS is described in Fig. 7. The main data of this WECS are presented in table 1, including an approach for the power coefficient obtained from the blade geometry. To compute the parameters of the nominal model, the effective average wind speed is considered as 7m/s.

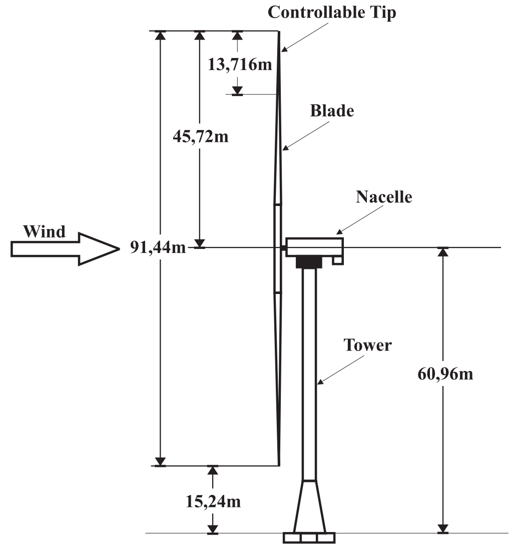

Figure 6. Sketch of HAWT used herein.

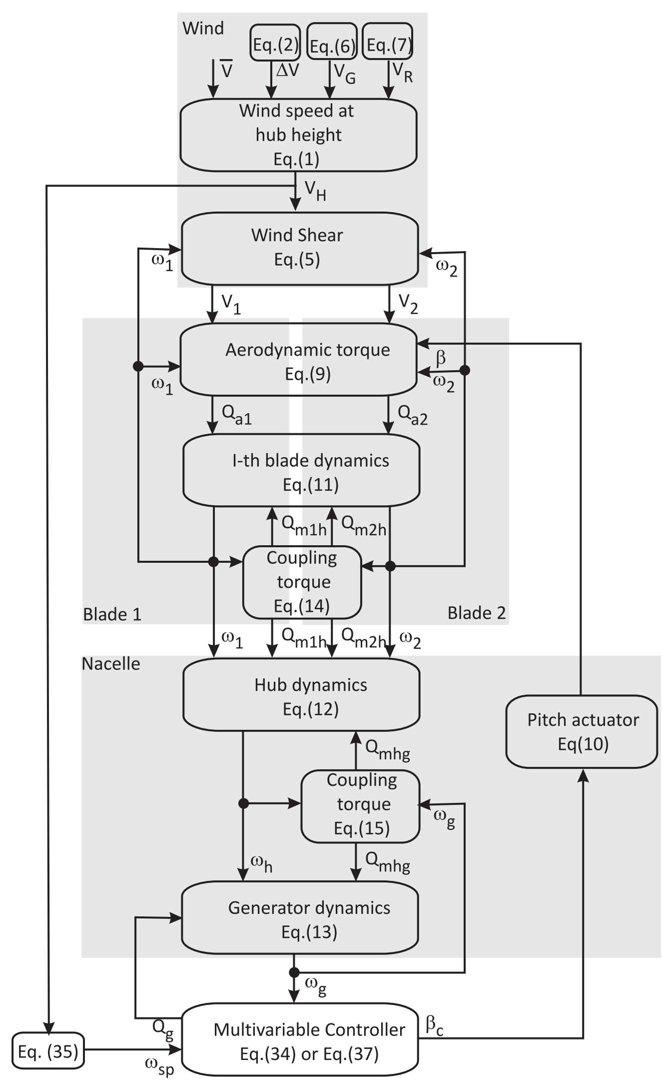

Figure 7. Block diagram of the dynamic simulation of the WECS control.

Table 1. WECS data.

Limits		
cut-in wind speed	cut-off wind speed	rated wind speed
5.8 m/s	20 m/s	12.5 m/s
Normalized Parameters of WT Base values: P_{base} = 2.5MVA and S_{base} = 17.55RPM		
Drive Train Parameters		
Normalized Inertias (J_{base} = 740165 kg.m^2)		
$J_{B1} = 18.23$	$J_{B2} = 18.23$	$J_H = 0.9527$
$J_t = J_{B1} + J_{B2} + J_H = 37.4127$		
$J_G = 2.091$		
Normalized Stiffness Constants ($\omega_{base}K_{base}$ = 1360299 kg.m^2/s^3)		
$\omega_{base}K_{B1H} = 861.1$	$\omega_{base}K_{B2H} = 861.1$	$\omega_{base}K_{HG}$=28.4
Normalized Damping Constants ($\omega_{base}D_{base}$=1360299 kg.m^2/s^2)		
$\omega_{base}D_{B1} = 4.58 \times 10^{-3}$	$\omega_{base}D_{B2} = 4.58 \times 10^{-3}$	$\omega_{base}D_H = 1.108 \times 10^{-2}$
$\omega_{base}D_t = \omega_{base}D_{B1} + \omega_{base}D_{B2} + \omega_{base}D_H = 2.024 \times 10^{-2}$		
$\omega_{base}d_{B1H} = 29.31$	$\omega_{base}d_{B2H} = 29.31$	$\omega_{based}d_{HG} = 1.832$
$\omega_{base}D_g = 3.01 \times 10^{-2}$		
Power Coefficient		
$C_p = \frac{1}{2}\left(\frac{R}{\lambda} - 0.0022\beta^2 - 5.6\right)\exp\left(-0.17\frac{R}{\lambda}\right)$		
Servo-hydraulic Pitch Actuator		
$\tau = 0.032\ s$	$\xi = 1$	
Linearized Aerodynamic Parameters		
α = 7.6949kg.m/s	γ = -16.1814kg.m^2/rad.s	κ = -144.5773kg.m^2/rad.s^2
Weighting Functions		
$K_\delta = 5$	$K_q = 1$	$K_\beta = 10$
$K_e(s) = 1.5 + \frac{1}{s}$		

The frequency response of the open-loop WECS is shown in Fig. 8. Although high frequency wind fluctuations are well rejected, WECS is very affected by low frequency wind disturbances. It is noted that the control input β is more effective on WT regulation than Q_g, although it reduces energy conversion efficiency. Torsional modes can be excited by sudden wind variations and/or operational disturbances since this WECS presents a resonance peak on:

$$\omega_{res} = \sqrt{K_{hg}\left(\frac{1}{J_t} + \frac{1}{J_g}\right)} = 1.9752\ rad/s \tag{41}$$

H_2 Controller Performance

Considering the WECS presented in the subsection "Plant Description", the use of the H_2 design procedure results in the following controller:

$$\mathbf{K}_2(s) = \begin{bmatrix} \dfrac{0.07592s^4 - 0.6462s^3 - 3.923s^2 - 2.761s - 0.7238}{s^5 + 4.504s^4 + 11.09s^3 + 13.27s^2 + 7.454s + 7.547x10^{-6}} \\ \dfrac{-0.2345s^4 - 0.6949s^3 - 1.269s^2 - 0.5969s - 0.07599}{s^5 + 4.504s^4 + 11.09s^3 + 13.27s^2 + 7.454s + 7.547x10^{-6}} \end{bmatrix}$$

The frequency response of the closed-loop WECS with an H_2 controller is shown in Fig. 9. High frequency wind fluctuations are submitted to strong attenuation. For frequencies below 0.7 rad/s, the sensitivity function (e_t/ω_{sp}) decays rapidly when the frequency tends to zero, as shown in its Bode plots, satisfying the requirements related to disturbance rejections. Bode plots of the complementary sensitivity function ($\omega_g/\ \omega_{sp}$) show that the H_2 controller attenuates measurements noise above 0.7 rad/s, assuring good robustness against uncertainties above this frequency. In regards to the rotation difference $\Delta\omega$, the excitation of torsional modes is difficult due to an adequate attenuation of reference variations and/or operational disturbances. Although power fluctuations on the electric load are attenuated, the system's response to variations of the electric torque Q_g will be slow.

The simulation results presented in Fig. 10 show the dynamic behavior of the fixed-speed closed-loop WECS when submitted to a wind gust with duration of 90 s. After this event, both control inputs are simultaneously used in the rotation regulation, and ω_t returns to its reference value ω_{sp} after approximately 5 minutes. Considering a variable speed operation, the rotation reference must be adjusted to:

$$\omega_{sp} = \frac{\lambda_{opt}}{R}V \tag{42}$$

The simulation results presented in Fig. 11 verify the effect of a wind step variation of 7.5 m/s to 9.5 m/s in the dynamic behavior of the variable-speed closed-loop WECS. In this case, ω_t follows speed reference ω_{sp}, reaching zero error after 10 minutes. Aiming to adjust ω_t, the generator torque Q_g is practically duplicated, increasing the energy delivered to the electric load. Considering that β has a detrimental effect on energy conversion efficiency, the relatively small contribution of this control input on rotation regulation is positive for variable speed WECS. The system's operation does not excite any torsional modes and the noises introduced by wind fluctuation are filtered by the H_2 controller.

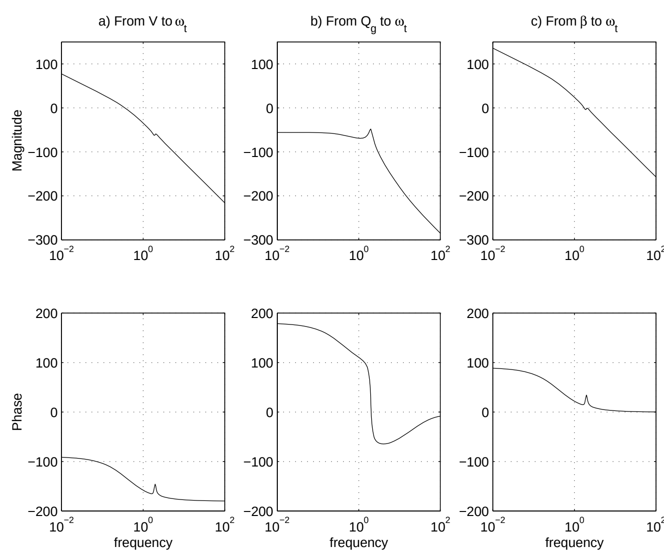

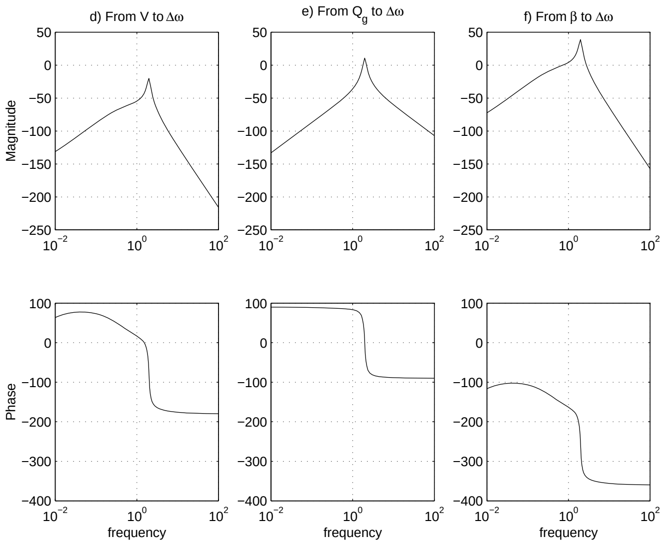

Figure 8. Bode plots of linearized open-loop WECS model.

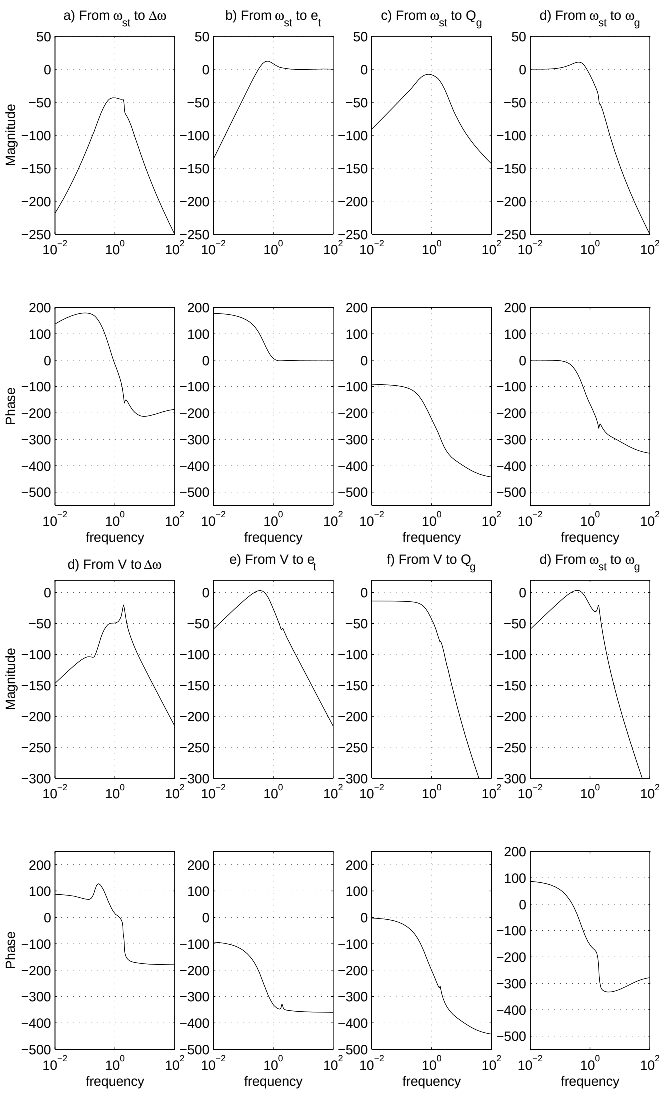

Figure 9. Bode plots of H_2 closed-loop WECS.

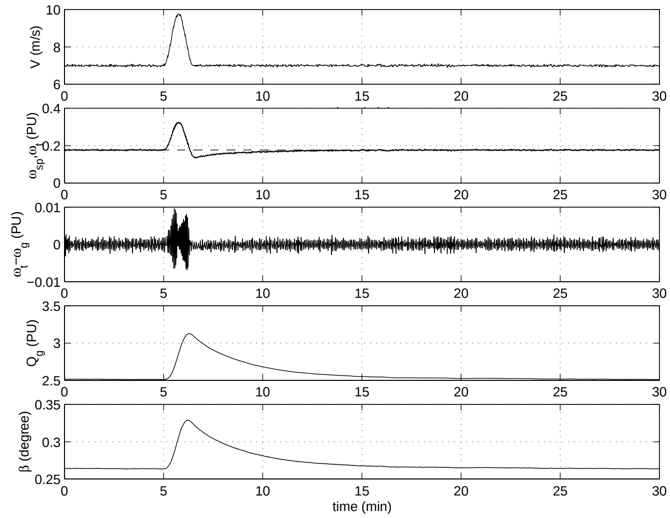

Figure 10. H_2 closed-loop WECS at fixed-speed operation: wind gust.

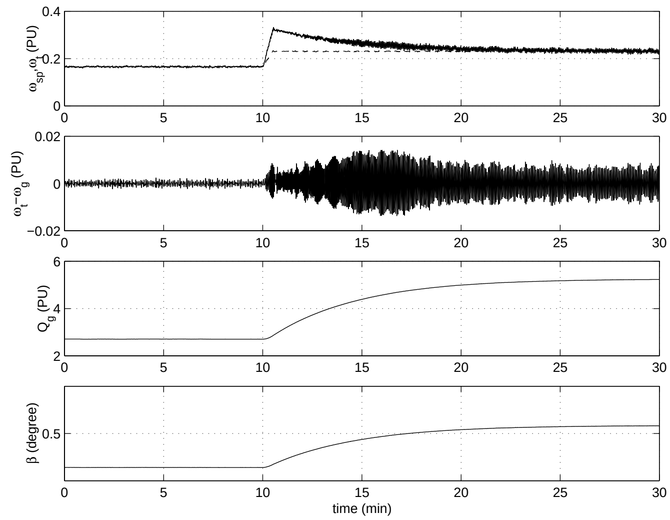

Figure 11. H_2 closed-loop WECS at variable-speed operation: wind step.

H_∞ Controller Performance

Considering the WECS presented in the subsection "Plant Description", the optimal H_∞ controller is obtained with $\varepsilon = 0.0674$:

$$\mathbf{K}_\infty(s) = \begin{bmatrix} \dfrac{2.297s^4 - 2.253\,s^3 - 8.93\,s^2 - 2.685s - 0.3474}{s^5 + 16.25\,s^4 + 52.89s^3 + 92.42s^2 + 51.75s + 5.18\text{x}\,10^{-5}} \\ \dfrac{-1.138s^4 - 3.18s^3 - 6.059s^2 - 2.58s - 0.22}{s^5 + 16.25s^4 + 52.89s^3 + 92.42s^2 + 51.75s + 5.18\text{x}\,10^{-5}} \end{bmatrix}$$

The frequency response of closed-loop WECS with the H_∞ controller is shown in Fig. 12. Notice that high frequency wind fluctuations are strongly attenuated. The sensitivity function decays rapidly for frequencies below 0.7 rad/s and the complementary sensitivity function is attenuated above 0.7 rad/s, assuring the requirements related to disturbance rejections and robustness against uncertainties. The H_∞ controller provides adequate attenuation of the reference variations or operational disturbances and, if compared to the H_2 controller, it provides a greatest attenuation for power fluctuations in the grid, resulting in an extremely slow response for variations on electric torque Q_g.

In relation to a fixed-speed operation, the dynamic behavior of the H_∞ closed-loop WECS when submitted to a wind gust with duration of 180 s is shown in Fig. 13. If compared with the H_2 controller, this controller presents better robustness, without unstable behavior when submitted to greatest disturbances. The control system is able to reject the effects of this wind disturbance using simultaneously β and Q_g. The turbine speed ω_t returns to its reference value ω_{sp} approximately at the end of the wind gust. The simulation results for variable speed closed-loop WECS when submitted to wind step variation from 7.5 m/s to 9.5m/s are shown in Fig. 14. Notice that the β performance on the rotation adjustment is improved. Although ω_t will eventually reach the reference ω_{sp}, this adjustment is extremely slow.

Conclusions

H_2 or H_∞ optimal feedback control problem involves finding a controller **K** for a generalized system **G**(s), using optimization techniques for the respective norms. Although both approaches present several similarities, the H_∞ methodology results in a more conservative controller than the H_2 methodology, since the disturbance signal dependency is considered in the H_∞ controller design. Thus, the H_∞ controller presents a better robustness than a similar H_2 controller, but its dynamic response is extremely slow. Although the H_∞ solution can be relatively flexible, admitting sub-optimal controllers, the tendency is to use the H_∞ controller in applications involving regulation problems, such as fixed-speed closed-loop WECS, where the output has to stay at determined value despite the presence of great disturbances. In counterpart, the fast response of the H_2 controller is more adequate for applications involving tracking problems, such as variable-speed closed-loop WECS, since it is necessary to follow a reference imposed by the wind speed to obtain maximum energy conversion. In this context, an interesting option for WECS controller designs can be the multi-objective H_2/H_∞ optimal control approach, where several channels associated with different norms are established, aiming to simultaneously attend several performance criteria.

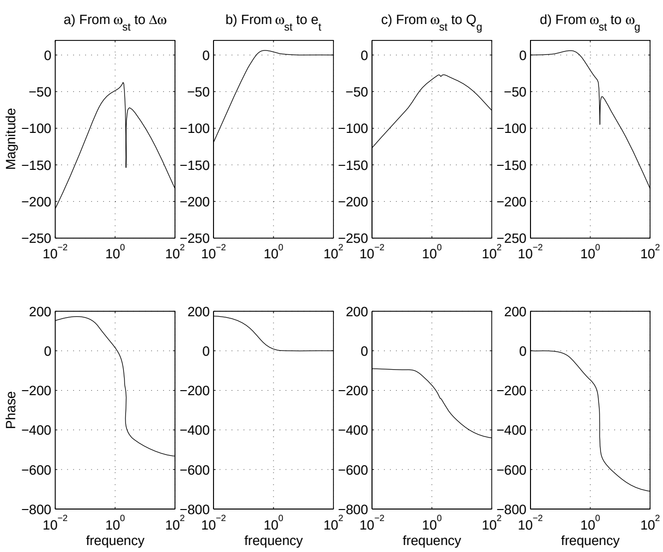

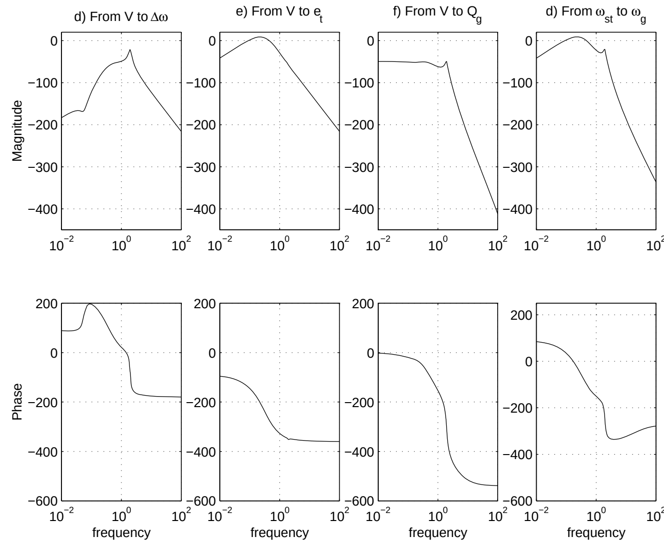

Figure 12. Bode plots of H_∞ closed-loop WECS.

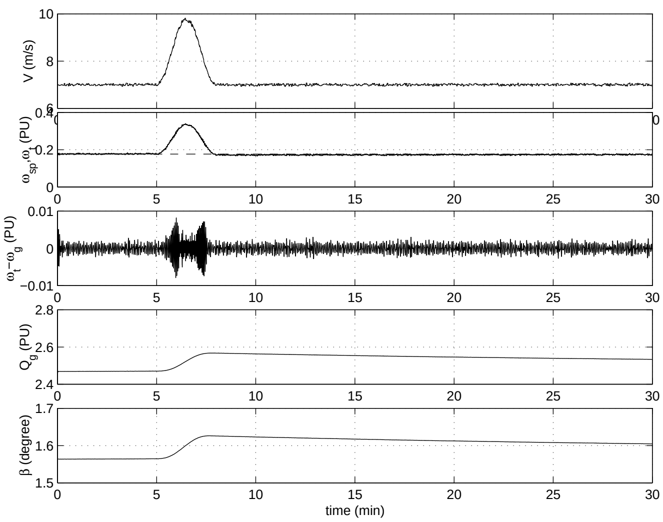

Figure 13. H_∞ closed-loop WECS at fixed-speed operation: wind gust.

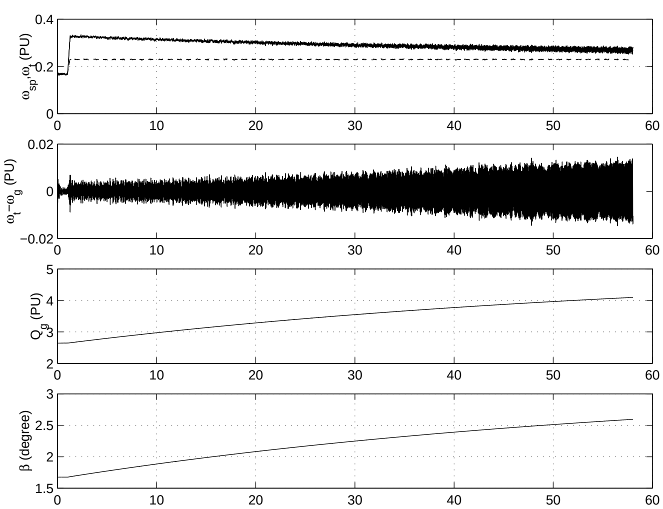

Figure 14. H_∞ closed-loop WECS at variable-speed operation: wind step.

References

Anderson, P.M. and Bose, A., 1983, "Stability simulation of wind turbine systems", *IEEE Trans. on Power Apparatus and Systems*, Vol. 102, No. 12, pp. 3791-3795.

Chang, R.Y., and Safonov M.G., 1996, "Robust control toolbox for use with matlab", Mathworks Inc., USA.

Dessaint, L., Nakra, H., and Mukhedkar, D., 1986, "Propagation and elimination of torque ripple in a wind energy conversion system", *IEEE Trans. on Energy Conversion*, Vol. 1, No. 2, pp. 104-112.

Doyle, J.C., Glover, K., Khargonekar, P.P., and Francis, B.A., 1989, "State-space solutions to standart H_2 and H_∞ control problems", *IEEE Trans. on Automatic Control*, Vol. 34, No. 8, pp. 831-846.

Freris, LL., 1990, "Wind Energy Conversion Systems", Prentice Hall Inc., United King.

Golding, E.W., 1977, "The Generation of Electricity by Wind Power", E. & F. N. Spon LTD, United King.

Hori, Y., Sawada, H., and Chun, Y., 1999, "Slow resonance ratio control for vibration suppression and disturbance rejection in torsional system", *IEEE Trans. on Industrial Electronics*, Vol. 46, No. 1, pp. 162-168.

Hwang, H.H., and Gilbert, L.J., 1978, "Synchronization of wind turbine generators against an infinite bus under gusting wind conditions", *IEEE Trans. on Power Apparatus and Systems*, Vol. 97, No. 2, pp. 536-544.

Johnson, C.C. and, Smith R.T., 1976, "Dynamics of wind generators on eletric utility networks", *IEEE Trans. on Aerospace and Eletronics Systems*, Vol. 12, No. 4, pp. 483-493.

Lefevbre, S. and, Dubé, B., 1988, "Control system analysis and design for an aerogenerator with eigenvalue methods", *IEEE Trans. on Power Systems*, Vol. 3, No. 4, pp. 1600-1608.

Leith, D.J., and Leithead, W., 1997, "Implementation of wind turbine controllers", *International Journal of Control*, Vol. 66, No. 3, pp. 349-380.

Leithead, W.E., de la Salle, S., and Reardon, D., 1991, "Role and objectives of control for wind turbines", *IEE proceedings-C*, Vol. 138, No. 2, pp. 135-148.

Maciejowski, J.M., 1989, "Multivariable Feedback Design", Addison-Wesley Publishing Company Inc., England.

Medeiros, A., Simões, F.J., Lima, A.M.N., and Jacobina, C.B., 1996, "Modelagem aerodinâmica de turbinas eólicas de passo variável", Proceeding od VI ENCIT / VI LATCYM, ABCM. Florianópolis, Brazil, pp. 25-30.

Novak, P., Ekelund, T., Jovik, I., and Schmidtbauer, B., 1995, "Modeling and control of variable speed wind-turbine drive-system dynamics", *IEEE Control Systems*, Vol. 15, No. 4, pp. 28-38.

Raina, G., and Malik, O.P., 1985, "Variable speed wind energy conversion using synchronous machine", *IEEE Trans. on Aerospace and Electronic Systems*, Vol. 21, No. 1, pp. 100-104.

Rocha, R., and Martins Filho, L.S., 2003, "A multivariable H_∞ control for wind energy conversion system", Proceedins of IEEE Conference on Control Applications, Istambul, Turkey.

Rocha, R., Resende, P., Silvino, J.L., and Bortolus, M.V., 2001, "Control of stall regulated wind turbine through H_∞ loop shaping methods", Proceedings of IEEE Conference on Control Applications, Mexico City, Mexico.

Rohatgi, J., and Pereira, A., 1996, "Modeling wind turbulence for the design of large wind turbines – a preliminary analysis", Proceedings of IV CEM-NNE, pp. 735-739.

Skogestad, A., and Postlethwaite, I., 2001, "Multivariable Feedback Control – Analysis and Design", John Wiley and Sons.

Wasynczuk, O., Man, D.T., and Sullivan, J.P., 1981, "Dynamic behaviour of a class of wind turbine generators during random wind fluctuatons", *IEEE Trans. on Power Apparatus and Systems*, Vol. 100, No. 6, pp. 2837-2845.